Axial Load-Transfer Curves for Suction Bucket Foundations in Sand

Grecu, Sorin; Barari, Amin; Ibsen, Lars Bo

Published in:
The Proceedings of The Twenty-ninth (2019) International Offshore and Polar Engineering Conference

Publication date:
2019

Document Version
Other version

Proceedings of the Twenty-ninth (2019) International Ocean and Polar Engineering Conference **www.isope.org**
Honolulu, Hawaii, USA, June 16-21, 2019

ISBN 978-1 880653 85-2; ISSN 1098-6189

Axial Load-Transfer Curves for Suction Bucket Foundations in Sand

Sorin Grecu, Amin Barari and Lars Bo Ibsen
Department of Civil Engineering, Aalborg University
Aalborg, Denmark

ABSTRACT

Multi-footed structures resting on suction buckets (suction caissons) comprise a promising foundation solution for next-generation 10 MW+ offshore wind turbines located in transitional water depths. For such systems, predicting the axial behavior of buckets is a critical design aspect. Load-transfer or *t–z* curves have been employed for decades as an efficient tool in pile design, however applying existing formulations to suction buckets bears uncertainty. This paper introduces a novel family of static *t–z* curves (Winkler springs) for suction buckets installed in typical marine sand. The study is based on 50 finite-element models that involve various foundation dimensions and soil properties, as well as drained uplift and compression. The non-linear springs' properties are therefore linked to suction bucket diameter, friction angle and vertical overburden pressure. Lastly, good agreement is found between the current results and the ones from other numerical studies. Since the proposed *t–z* curves require only three basic parameters, they may be conveniently implemented in preliminary stages of foundation design.

KEY WORDS: suction bucket; t–z curves; numerical modeling; friction; offshore foundation; sand.

INTRODUCTION

Efforts to increase feasibility of offshore wind energy are reflected by a general tendency towards installing high-capacity 10MW+ offshore wind turbines (OWTs) further from coastlines (Wang et al., 2018), which typically involves larger water depths and larger resultant moments (Larsen et al., 2013; Ibsen et al., 2014). Such endeavors give rise to new technical challenges associated with design, installation and performance of OWT foundations. Large-diameter hollow steel columns (monopiles) represent the commonly adopted solution in shallow waters up to 30 m deep. However, monopiles become impractical at larger depths, rendering the well-established expertise trivial. In light of this fact, interdisciplinary studies on new foundation methods are crucial for the development of offshore wind industry.

A promising foundation concept for OWTs in transitional water depths (30–60 m) consists of a three- or four-legged jacket structure mounted on suction buckets (Oh et al., 2018). The idea of suction bucket is borrowed from the oil & gas sector, where this technology is widely used for anchoring floating platforms (Tjelta, 2015). Unfortunately, the current practices cannot ensure optimal design of suction buckets for OWTs, due to differences in loading patterns. As opposed to oil/gas platforms, offshore wind structures are significantly lighter, therefore the horizontal loading component becomes an essential design issue.

Fig. 1(a) illustrates the load transfer mechanism in a typical jacket structure. Environmental loads generate an overturning moment that triggers a "push–pull" mechanism whereby individual buckets are axially loaded either in tension or compression. Thus, overall stability is closely connected to axial response of suction buckets. In this paper, focus is placed on friction between bucket skirt and adjacent soil during vertical monotonic drained loading (see Fig. 1(b) and Fig. 1(c)).

A commonly adopted method for modeling soil–structure interaction is the Winkler approach (Winkler, 1867). Its principle lies in idealization of the structure into discrete elements, where each of them is attached to a non-linear spring that simulates soil reaction at any given vertical deflection of its associated element (see Fig. 2). The behavior of each spring is described by a relationship between shear stress in the soil medium in immediate proximity to the structure, τ, and relative soil–structure vertical displacement, z. The graphical representation of this relationship is referred to as "*t–z* curve" or "load-transfer curve".

Load-transfer curves comprise a convenient means to assess axial behavior of piles. In fact, all existing *t–z* formulations relate strictly to deep slender substructures. The majority of proposed relationships were derived empirically from test data or analytically from theoretical considerations (Seed and Reese, 1957; Coyle and Sulaiman, 1967; Vijayvergiya, 1977; Randolph and Wroth, 1978; Kraft et al., 1981; Fleming, 1992; Wang et al., 2012; Nanda and Patra, 2014; Bohn et al., 2016; Zhou et al., 2019). The success of the Winkler method is explained by its capability to account for soil's inherent non-linearity and for random layer distribution while exhibiting relative mathematical ease (Lombardi et al., 2017).

The motivation for the current study stems from the idea that existing *t–z* curves are prone to misrepresenting the frictional response of suction buckets subjected to axial loading. The unreliability of applying pile-

specific curves to buckets is rooted in notable differences between behaviors of the two foundation types. Suction buckets have relatively small length-to-diameter ratios and embedment depths, and thus their associated failure mechanisms exhibit features related to shallow footings and to piles. Moreover, internal mechanisms develop within entrapped soil and their effects on internal skirt friction cannot be ignored.

This paper proposes a novel set of *t–z* curves for suction buckets installed in cohesionless soil based on numerical modeling. The set consists of two distinct formulations defined according to two loading scenarios: uplift and compression. The loading direction determines the failure mechanism, as described by Mana et al. (2012) in their discussion of centrifuge test results, which in turn reflects upon the development of skirt friction. This justifies the necessity of formulating *t–z* curves for each loading direction separately.

The advantage of the proposed load-transfer curves lies in their straightforward formulation in terms of bucket diameter, D, initial effective vertical overburden pressure, σ'_{v0}, and friction angle, ϕ, of sand. The last two variables are basic geotechnical parameters that can be obtained from conventional tests. Within the Limit State Design approach, the non-linear axial springs play a significant role in Ultimate Limit State (ULS) checks. The contribution of skirt friction to the vertical capacity of the foundation may be estimated by constructing load–displacement relationships based on *t–z* curves and identifying the threshold associated with a given criterion.

Since only monotonic loading is considered in the present study, the derived *t–z* curves are static, i.e. they do not incorporate the effects of cyclic and dynamic loading. Nonetheless, the proposed load-transfer relationships can be implemented in the analysis of target natural frequency of the system. This is an essential aspect of OWT design, as these structures are continuously subjected to harmonic excitation.

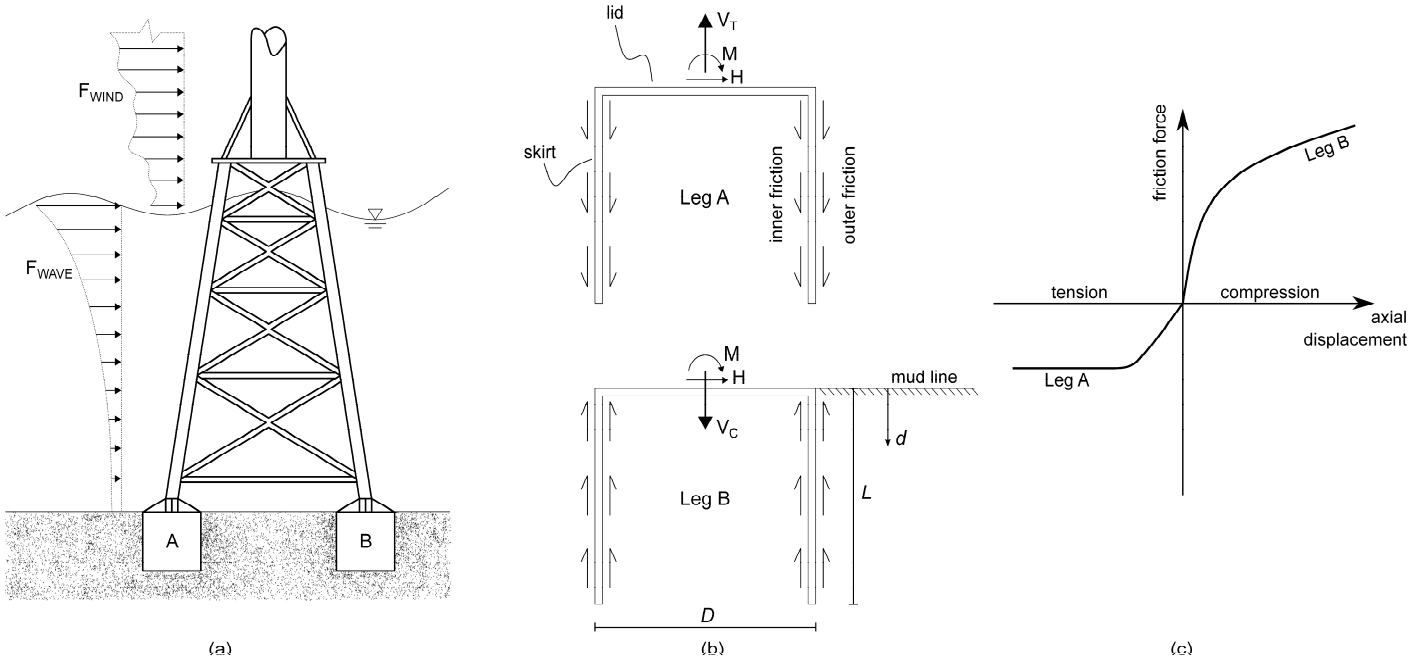

Fig. 1. (a) Schematic elevation of a four-legged jacket structure resting on suction buckets; (b) Skin friction contributes to the stability of the system by counteracting the imposed vertical loads. Other stabilizing factors are purposely omitted in the sketch; (c) The loading direction plays a major role in the frictional behavior of suction buckets

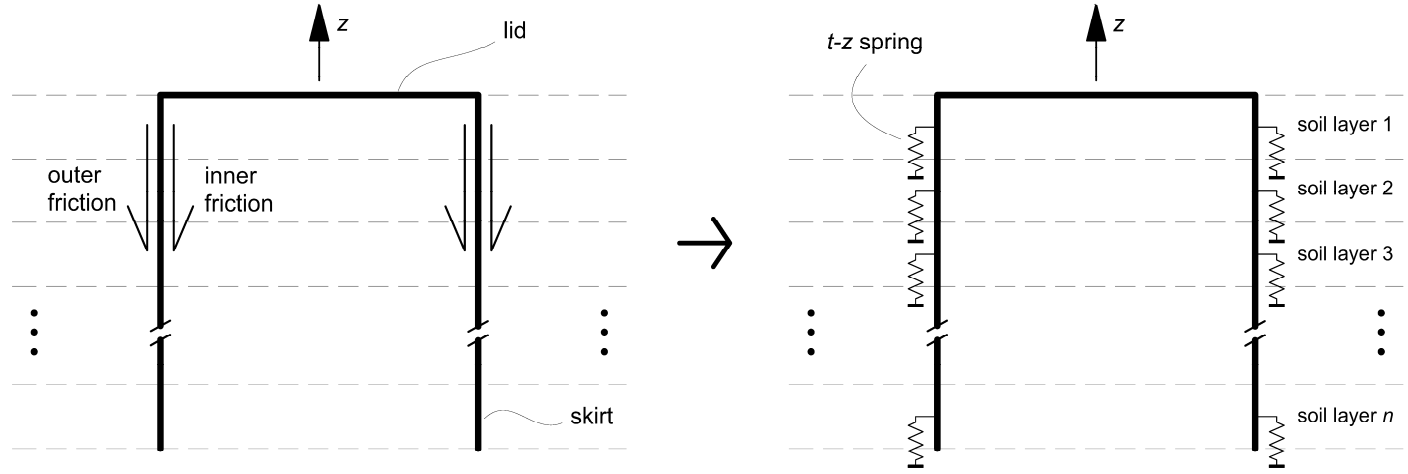

Fig. 2. Idealization of the system whereby soil–structure interaction is represented by axial springs

The new *t–z* formulations are verified by comparison with results from relevant numerical studies and with pile-specific relationships given by design codes.

NUMERICAL MODELING

Research involving numerical simulations of suction bucket foundations by means of finite-element (FE) method illustrates the technique's efficacy and convenience for assessing the behavior of the system (Barari and Ibsen, 2012; Achmus et al., 2013; Achmus and Thieken, 2014; Mana et al., 2014; Thieken et al., 2014; Østergaard et al., 2015; Achmus and Gütz, 2016; Park et al., 2016; Park and Park, 2017; Sørensen et al., 2016; Shen et al., 2017; Lu and Luo, 2018; Barari and Ibsen, 2018). On grounds of conceptually identical purposes, this paper along with two other companion papers by researchers at Aalborg University, Østergaard et al. (2015) and Vahdatirad et al. (2016), develops a generalized Winkler-type model by a set of two axial springs.

Single buckets subjected to axial loading and installed in uniform sand were modeled. The computation time was significantly reduced by taking advantage of the system's cylindrical symmetry. It is worth noting that the adopted approach excludes the possibility of accounting for group effects present in multi-footed foundations.

In total, 50 axisymmetric finite-element models were constructed with Plaxis 2D (Plaxis, 2017). Each model comprised a combination of various input parameters, which are described in the following list.

- Bucket dimensions: lid diameter, D, and skirt length, L. The aspect ratio was equal to unity in all models. Keeping in mind the potential size of suction buckets supporting jacket structures, the following values for D and L were used: 10, 13, 15, 18 and 20 m.
- The angle of internal friction, ϕ, was implemented as an independent variable dictating the properties of Frederikshavn sand, i.e. all soil parameters were defined as functions of ϕ. The process of establishing these functions is explained later in the paper. Five friction angles were considered: 30°, 33°, 35°, 38° and 40°.
- Displacement direction was defined as either monotonic upwards (tensile loading) or downwards movement (compressive loading).

Fig. 3 illustrates the mesh composed of triangular fifteen-node quartic elements and the domain extents relative to bucket dimensions. The mesh around the bucket was refined in order to obtain a clear picture of stress distribution in the region of interest, where gradients are largest. A convergence study gave the optimal degree of local *h*-refinement. The procedure involved examining soil–structure interface shear stress changes with respect to a gradually increasing number of elements. Concurrently, a domain size analysis ensured that the model edge effects became negligible, in the context of simulating realistic site conditions.

The nodes along the axis of symmetry and along the opposite edge were horizontally restrained, while the bottom edge was fully fixed. Vertical displacements were prescribed to all nodes in elements that defined the bucket, whilst restricting horizontal deflections thereof. It is stressed that prescribed displacements were assigned to the embedded part of the foundation as well, under the assumption of a structure exhibiting rigid body behavior.

The numerical analyses followed the following steps to simulate actual field conditions:

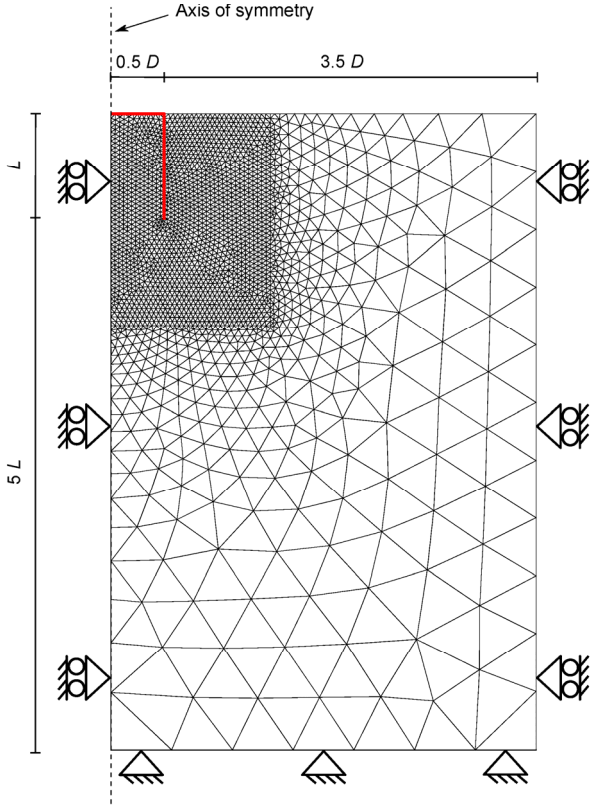

Fig. 3. FE model set-up. The bucket is highlighted in red

1) *K0* procedure: soil initially undergoes geostatic stresses.
2) Foundation and interface elements: a part of soil is replaced by the foundation. The caisson analysis does not address the construction process, which means the foundation is "wished-in-place". In practice, the soil softening phenomenon associated with the installation process is unavoidable, but it can be accounted for by modifying the soil strength and stiffness parameters accordingly (Hossain and Randolph, 2009). Nevertheless, Achmus et al. (2013) and Zafeirakos and Gerolymos (2016) assumed that installation effect is of minor importance regarding the general bucket performance and its degrading influence was therefore disregarded in their analyses.
3) Nil-step phase: displacements and small strains due to activation of the structure are reset to zero.
4) Loading phase: prescribed displacements are applied to the bucket.

Material Modeling and Properties

The Hardening Soil model (Schanz et al., 1999) with small-strain stiffness (HSsmall) defined the constitutive relationships for cohesionless soil, with input parameter values related to Frederikshavn sand at various compaction states.

Firstly, the link between relative density, D_r, and friction angle, ϕ, is established by rearrangement of empirical relationships derived by Bolton (1986), and is expressed by

$$D_r = \frac{\phi - \phi_{crit} + 3R + \Delta\phi_1}{3\left(Q_{min} - \ln\frac{p'}{1\ \text{kPa}}\right) - 3} \quad (1)$$

where ϕ_{crit}=33° is the critical friction angle; $\Delta\phi_1$=2° is the correction corresponding to 5–10% of silt content; Q_{min}=10 is a coefficient related to quartz sands; p'=100 kPa is the reference effective mean stress; and R=1 is a fitting coefficient. The initial void ratio, e, can be computed by using the definition of D_r. According to Nielsen et al. (2012), the minimum e_{min} and maximum e_{max} void ratios of Frederikshavn sand are equal to 0.64 and 1.05, respectively.

Based on Janbu's tangent modulus concept (Janbu, 1967), outlined in DNV (1992), the reference oedometer modulus, E_{oed}^{ref}, is formulated in terms of D_r as follows

$$E_{oed}^{ref} = 16142D_r^2 + 19987D_r + 3688 \quad \text{[in kPa]} \tag{2}$$

where the superscript denotes the modulus at a reference confining stress σ_{ref}=100 kPa. The coefficients in Eq. 2 are found by means of regression analysis of data related to Norwegian inorganic sands, presented in DNV (1992).

Adhering to theory of elasticity, it is roughly assumed that the reference secant modulus, E_{50}^{ref}, depends on E_{oed}^{ref} in the following manner

$$E_{50}^{ref} = \frac{1-\nu-2\nu^2}{1-\nu} E_{oed}^{ref} \tag{3}$$

which implies equivalence between E_{50}^{ref} and Young's modulus, E. Poisson's ratio, ν, can be computed according to

$$\nu = \frac{1-\sin\phi}{2-\sin\phi} \tag{4}$$

The reference unload/reload modulus is estimated as $E_{ur}^{ref}=3E_{50}^{ref}$. The dependency of soil stiffness on confining stress is accounted for in the Hardening Soil model, as described by Schanz et al. (1999). For the sake of brevity, the relationships between reference moduli, which act as input parameters, and calculated stress-dependent moduli are not presented in this paper.

Two additional parameters are required to model small-strain stiffness: reference shear modulus at very small strains ($\varepsilon < 10^{-6}$), G_0^{ref}, and threshold shear strain, $\gamma_{0.7}$, at which the reference secant shear modulus $G_s^{ref} = 0.722G_0^{ref}$. According to Hardin and Black (1969), the former may be estimated as

$$G_0^{ref} = 33\frac{(2.97-e)^2}{1+e} \quad \text{[in MPa]} \tag{5}$$

The threshold shear strain, $\gamma_{0.7}$, is computed as follows

$$\gamma_{0.7} = \frac{2c'(1+\cos 2\phi) - \sigma_v'(1+K_0)\sin 2\phi}{9G_0^{ref}} \tag{6}$$

where effective cohesion c' = 0.1 kPa; earth pressure coefficient at rest $K_0 = 1-\sin\phi$; and σ_v' is the effective vertical stress.

The interface friction angle, δ, is assumed as 2/3 of ϕ, adopting indicative values specified by API (2000) and following other numerical studies (Achmus et al., 2009, 2013; Park et al., 2016). The dilation angle, ψ, is defined by $\phi - \phi_{crit}$, as suggested by Bolton (1986). Table 1 summarizes all five sets of soil parameters used for numerical modeling, where each set corresponds to a chosen friction angle.

Table 1. Soil parameters used in the FE models

Parameter: unit	Set 1	Set 2	Set 3	Set 4	Set 5
ϕ: degrees	30	33	35	38	40
D_r: %	15.2	37.9	53.1	75.8	91.0
e	0.99	0.89	0.83	0.74	0.68
ψ: degrees	0	0	2	5	7
γ_{sat}: kN/m^3	18.3	18.7	19.0	19.4	19.8
γ_{dry}: kN/m^3	13.3	13.9	14.4	15.2	15.7
E_{50}^{ref}: kPa	4727	9717	14044	22129	28622
E_{oed}^{ref}: kPa	7091	13589	18849	28133	35251
E_{ur}^{ref}: kPa	14182	29150	42131	66387	85867
m	0.5	0.5	0.5	0.5	0.5
G_0^{ref}: kPa	65228	75034	82300	94449	103490
$\gamma_{0.7}$: 10^{-3} m/m	0.2218	0.1973	0.1813	0.1583	0.1438
ν	0.33	0.31	0.30	0.28	0.26
K_0	0.5	0.46	0.43	0.38	0.36
δ: degrees	20	22	23.3	25.3	26.6

Rigid body properties were attributed to the modeled bucket, in order to reduce the influence of structural deformations on soil response. This assumption was enforced in two steps: (*a*) by prescribing displacements to all structural elements, including those that model the bucket skirt; (*b*) by deliberately setting a large elastic modulus of steel, thereby increasing the bending and axial stiffness of the structure.

The unit weight of water, γ_w, was set to 10 kN/m^3 and the gravitational acceleration to 9.81 m/s^2.

Qualitative Description of FE Results

In this subsection, results obtained from the numerical analyses are presented and discussed. The model with parameters D=L=15 m and ϕ=35° serves an illustrative purpose throughout the entire paper.

Within the analysis of soil–structure friction, the extracted data relates to shear stress extracted from interface elements, rather than from soil elements adjacent to the structure. This modeling framework follows a comparison study which confirmed that larger stresses occur in interfaces (Wolf et al., 2013). The interface stress points are grouped according to equally sized segments (hereafter referred to as "layers"). The stress values generated from points within a layer are averaged for every calculation step.

Fig. 4 shows plots of layer-averaged interface shear stress against vertical displacement of the structure in case of tensile and compressive loading. Each curve is linked to a mid-layer depth. Complex mechanisms and numerical instabilities affiliated with abruptly changing geometry (regions close to the bucket lid and the skirt tip) are represented by highly non-linear curves. The trends thereof deviate from the ones that reflect more elementary and predictable soil–structure interaction across the major part of skirt area. Therefore, these curves (shown in grey and black in Fig. 4) are disregarded in the forthcoming statistical analysis.

The bilinear curves depicted in Fig. 4(a) are identical with the ones recommended by API (2000) in that stress increases linearly until a peak value, τ_p, is reached ("pre-failure" part), after which it becomes constant ("post-failure" part). In drained conditions, the upwards movement of the

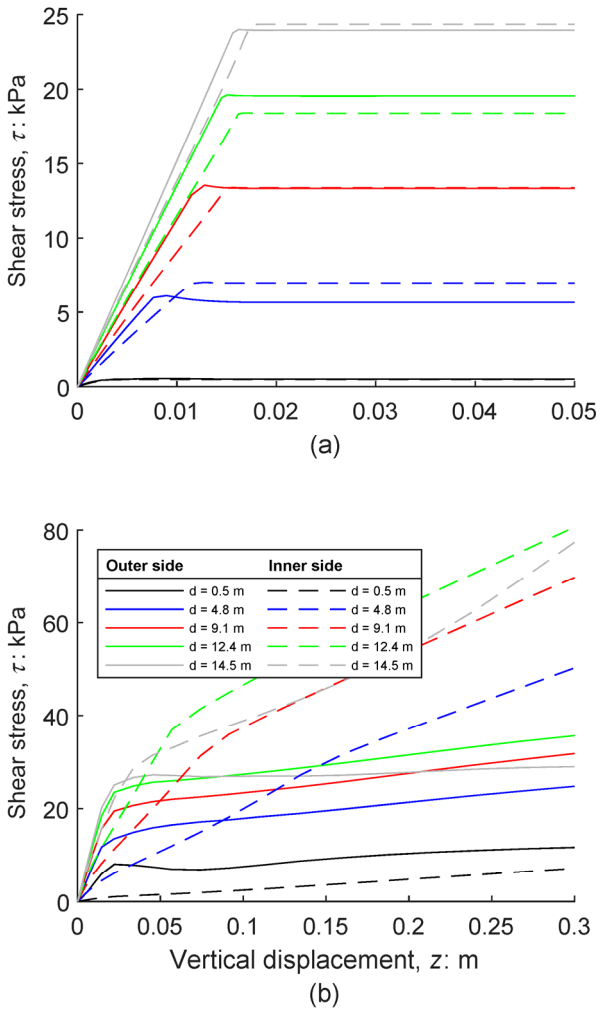

Fig. 4. Shear stress development in the soil–structure interface at various depths below mudline, d: (a) uplift; (b) compression

bucket leads to skin friction along inner and outer side of the skirt face developing in similar manners and contributing almost equally to axial resistance. The vertical displacement at which the peak stress occurs, z_p, increases non-linearly with depth. At the same time, such dependency is observed in terms of stiffness.

Regarding drained compressive loading, Fig. 4(b) reveals continuous stress growth without clear peaks along inner skirt. This behavior results from the bucket lid that acts as a surcharge on the entrapped soil mass, thereby gradually increasing the effective normal stress on the inner skirt area. The initial outer response resembles the one observed in case of drained tensile loading (cf. Fig. 4(a)), however the post-failure part is marked by linearly increasing stress.

FORMULATION OF T–Z CURVES FOR UPLIFT

Observing the curves presented in Fig. 4(a), three conclusions may be drawn with regards to formulating a general mathematical model of axial spring stiffness for buckets subjected to tension.

- It might prove convenient to study the total frictional response by superimposing the curves related to inner and outer skirt faces. Since the two responses are almost identical, the total effect is only expressed by a change in magnitude, while the curves' shapes are preserved.
- A piecewise function (Eq. 7) can be employed to represent bilinear curves, with its condition being established in connection with vertical displacements at which the peak shear stresses occur, z_p.
- Normalization with respect to τ_p and z_p can be applied so that all peaks are located at (1,1) in the τ/τ_p–z/z_p plane. The result is the complete alignment of curves related to all models. In this context, it becomes clear that the core goal is establishing general expressions for τ_p and z_p. For practicality, the expressions may include relevant readily-available parameters as variables, namely bucket diameter, D, in-situ effective vertical stress, σ'_{v0}, and friction angle, ϕ.

The t–z curve for representing the drained tensile response of suction buckets in sand is associated with the following function:

$$\frac{\tau}{\tau_p} = \begin{cases} \dfrac{z}{z_p} & \text{for} \quad \dfrac{z}{z_p} < 1 \\ 1 & \text{for} \quad \dfrac{z}{z_p} \geq 1 \end{cases} \tag{7}$$

Peak Shear Stress, τ_p, and Peak Displacement, z_p

It is worth noting that τ_p in Eq. 7 is the sum of inner and outer peak shear stresses, thus the resulting τ incorporates the effects of both skirt sides.

Regression analysis using data from the 25 numerical models that involve drained tension is performed in order to assess the dependency of τ_p and z_p on bucket geometry, sand strength and vertical overburden pressure. Examining Fig. 5, it is seen that a power law of the form $f(x) = Ax^B$ constitutes an appropriate function for fitting data regarding each model individually. The outcoming R^2-values fall within ranges of 0.99–1.00 and 0.79–0.98 in connection with fitting of τ_p and z_p, respectively. A number of 25 values for parameters A and B are obtained, which allows the investigation of A and B as functions of bucket diameter and friction angle. The expressions for τ_p and z_p can be written as

$$\tau_p = A_\tau^t(D,\phi)\left(\frac{\gamma' d^2}{D\tan\phi}\right)^{B_\tau^t(D,\phi)} \tag{8}$$

$$z_p = A_z^t(D,\phi)\left(\frac{\gamma' d^2}{\sigma_a}\right)^{B_z^t(D,\phi)} \tag{9}$$

where the subscripts denote the link to the corresponding dependent variable; the superscripts relate to the loading direction and σ_a=100 kPa is the atmospheric pressure.

Parameters A and B

The coefficients A_τ^t, A_z^t, B_τ^t and B_z^t are treated separately in a multivariable analysis to describe their relation to D and ϕ. To achieve unitless quantities, the former is normalized with respect to D_{ref} =15 m, while the friction angle is represented through its tangent. Bivariate first- or second-order polynomials are used for surface fitting. Table 2 displays the results of the parametric study.

An exception is made for B_τ^t, since it exhibits weak correlation with either D or ϕ and its values are bound between 0.5601 and 0.5717. Using the average B_τ^t = 0.5685 proves to introduce negligible error between the mathematical formulation of peak shear stress and the FE results (see Fig. 5(a)).

Table 2. Summary of β-coefficients for modeling the tensile response. Here $x=D/D_{ref}$ and $y=\tan\phi$

Parameter	Fitting function	β_1	β_2	β_3	β_4	β_5	R^2
A_τ^t	$f(x,y)=\beta_1+\beta_2 x+\beta_3 y$	-0.425	1.084	2.443	–	–	0.9819
A_z^t	$f(x,y)=\beta_1+\beta_2 x+\beta_3 y+\beta_4 xy+\beta_5 y^2$	0.140	0.045	-0.400	-0.043	0.279	0.9686
B_z^t	$f(x,y)=\beta_1+\beta_2 x+\beta_3 y$	0.349	-0.003	-0.266	–	–	0.8250

Upon normalizing the results by implementing the mathematical models of τ_p and z_p, the curves related to all numerical models and depths align adequately (see Fig. 6). This serves as confirmation of two aspects: (*a*) the statistical model shows high fidelity with respect to original FE results; (*b*) the chosen function (Eq. 7) is representative of frictional behavior given drained conditions during tensile loading.

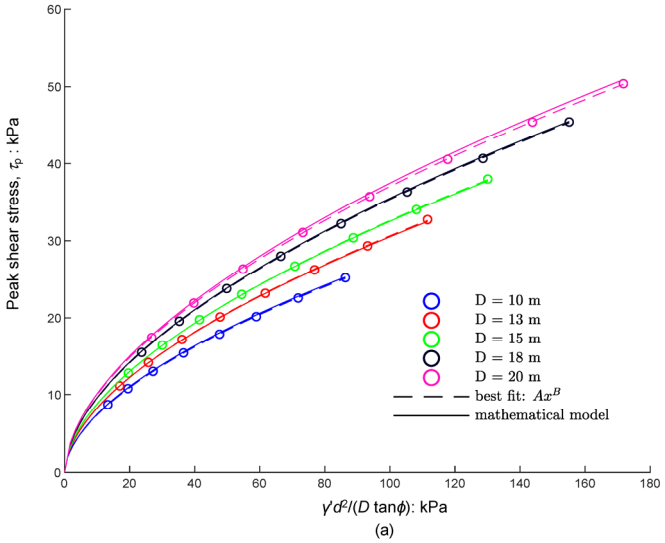

Fig. 5. Curve fitting of data from 5 models involving various bucket diameters and identical soil properties (marked by ϕ=35°) and estimations based on the established mathematical models: (a) peak shear stress, taken as the sum of inner and outer peak shear stresses; (b) displacements at which peak shear stresses occur

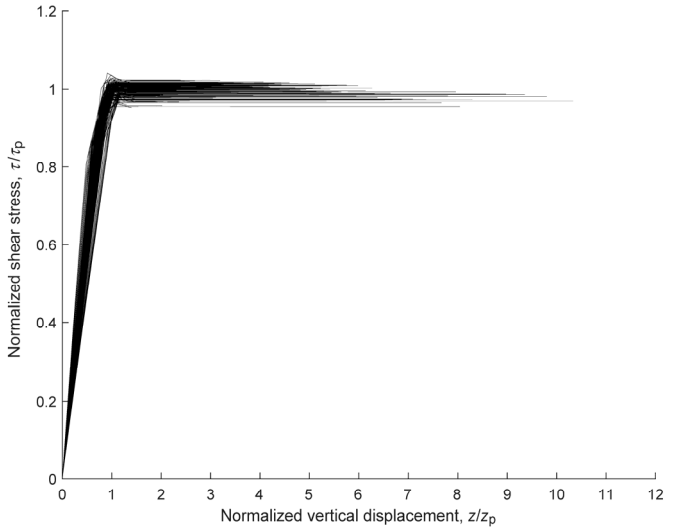

Fig. 6. Normalized *t–z* curves related to soil layers at various depths for all 25 FE models that consider buckets loaded in tension

FORMULATION OF T–Z CURVES FOR COMPRESSION

The following considerations stemming from Fig. 4(b) constitute the basis for modeling the frictional response of buckets under compression.

- Due to large discrepancies between developments of skin friction along inner and outer skirt, the two sides are treated individually, i.e. formulating a mathematical model for each side. Therefore, the total frictional response can be estimated by taking into account the inner and outer *t–z* springs simultaneously.
- Since failure occurs at the same displacement amplitudes at any depth within a numerical model, the vertical displacements may be normalized with respect to some constants, e.g. bucket diameter, *D*. The expressions for peak shear stress, τ_p, may be established by regression analysis according to the steps described earlier.
- Employing a single function, as opposed to a piecewise one, may suffice to accurately capture both pre- and post-failure responses, on grounds of relatively smooth transition between the two phases.

Inner Skirt Friction

Comparing the shear stress development at various depths (see Fig. 4(b)), it is seen that the representative curves differ not only in magnitude, but also in shape and degree of non-linearity. It becomes clear that a full alignment of normalized curves can only be achieved around delimited parts thereof. For example, using the maximum reached shear stress as a normalizing quantity yields adequate results in terms of aligning the curve tails, whereas significant divergence is present among other parts. Keeping in mind the practical design aspects and the level of working stress, priority is assigned to modeling the initial frictional behavior. Applying Eq. 10 (API, 2000) to compute the ultimate skin friction, τ_u,

leads to acceptable results regarding the normalization of the initial response (see Fig. 7).

$$\tau_u = \sigma'_{v0} K_0 \tan\delta \tag{10}$$

The data from each model is fitted with a power function, thus the mathematical model adopts the following form:

$$\frac{\tau}{\tau_u} = C_1^{in}(D,\phi)\left(\frac{z}{D}\right)^{C_2^{in}(D,\phi)} \tag{11}$$

where parameters C_1^{in} and C_2^{in} are studied as functions of bucket diameter and friction angle. The details of the study in question are given in Table 3.

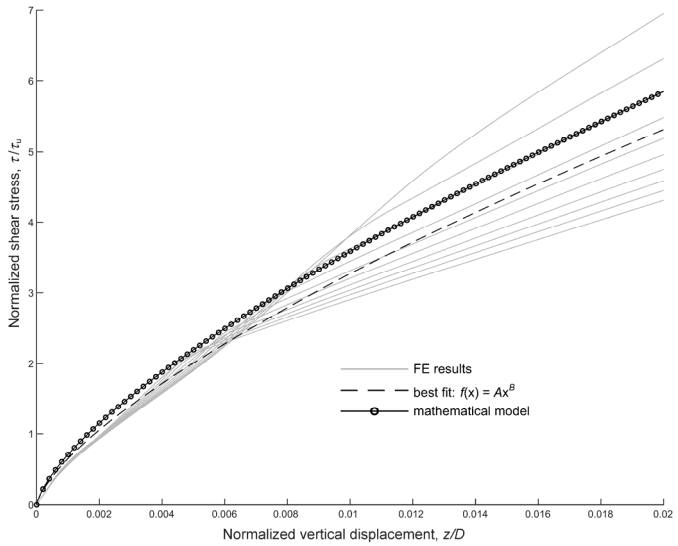

Fig. 7. Comparison between the normalized t–z curves at various depths below mudline and the proposed mathematical model for estimating friction on the inner side of the skirt during drained compressive loading. The example relates to the FE model where D=15 m and ϕ=35°

Outer Skirt Friction

An expression identical to the one seen in Eq. 8 is used for estimating the peak shear stress along outer skirt during drained compression. Table 3 displays the corresponding β-coefficients. The resulting value for τ_p is used in Eq. 12. A function composed of a hyperbolic tangent and a proportional term represents an acceptable candidate for fitting the normalized t–z curves for outer side of the skirt. The mathematical model can be expressed as follows:

$$\frac{\tau}{\tau_p} = C_1^{out}\tanh\left(C_2^{out}(\phi)\frac{z}{D}\right) + C_3^{out}(\phi)\frac{z}{D} \tag{12}$$

Regression analysis of C-coefficients yields sets of 25 values for each of them. Significant correlation with friction angle is found for C_2^{out} and C_3^{out}, while the mean value C_1^{out}=1.031 is used for the first coefficient.

$$C_2^{out} = 2632.1\tan\phi - 889.8 \tag{13}$$

$$C_3^{out} = 214.8\tan\phi - 116 \tag{14}$$

The best fit curves and the proposed t–z curves for modeling outer skirt friction during compression are illustrated in Fig. 8.

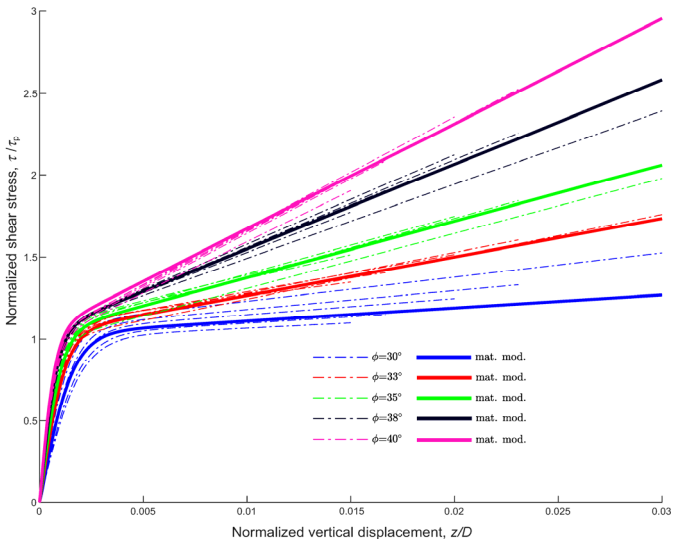

Fig. 8. Comparison between the best fit curves (dashed lines) from all numerical models and the proposed mathematical model curves for estimating friction on the outer side of the skirt during drained compressive loading

VALIDATION

Discretization of a foundation into a system of springs requires the assignment of layers (portions of the structure "replaced" by springs). Generally, accuracy increases with number of layers. The total frictional resistance, F_F, at any vertical displacement, z, is calculated by aggregating the effects of all layers in terms of their associated interface shear stresses.

$$F_F^t = \pi\frac{D^{out}+D^{in}}{2}\sum_{k=1}^{n} l_k\tau_k \tag{15}$$

$$F_F^c = \pi\sum_{k=1}^{n} l_k\left(D^{out}\tau_k^{out} + D^{in}\tau_k^{in}\right) \tag{16}$$

where F_F^t and F_F^c are the resulting frictional forces for uplift and compression, respectively; n is the number of layers; l_k is the thickness of the kth layer; D^{out} and D^{in} are the outer and inner diameters; τ is the shear stress arising during uplift, calculated with Eq. 7, and owing to its formulation, it incorporates both inner and outer friction; τ^{out} and τ^{in} are

Table 3. Summary of β-coefficients for modeling the compressive response. Here $x=D/D_{ref}$ and $y=\tan\phi$

Parameter	Fitting function	β_1	β_2	β_3	β_4	β_5	R^2
C_1^{in}	$f(x,y)=\beta_1+\beta_2x+\beta_3y+\beta_4x^2+\beta_5xy$	-522.5	156.1	1069.6	92.8	-547.1	0.9786
C_2^{in}		-0.200	0.437	1.362	0.093	-0.824	0.9654
A_τ^c	$f(x,y)=\beta_1+\beta_2x+\beta_3y+\beta_4xy+\beta_5y^2$	-3.97	6.933	-6.776	-7.916	25.7	0.9723
B_τ^c		1.124	-0.303	-1.48	0.547	0.276	0.9452

interface shear stresses along outer and inner skirt faces during compression, estimated with Eq. 12 and Eq. 11, respectively.

The load–displacement curves constructed with the proposed *t–z* curves are in close agreement with the ones computed directly from the numerical models (see Fig. 9). The errors stem from inaccuracies associated with regression analysis and with the assumption that shear stress development exhibits identical trends along the entire skirt face, including its extremities. The curves recommended by API (2000) yield conservative results for ultimate skin friction and predict earlier displacement at which it is reached.

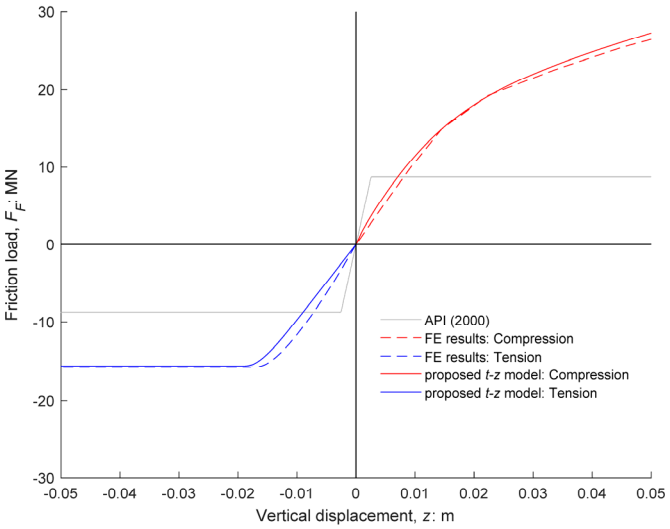

Fig. 9. Load–displacement curves. The example relates to the FE model where D=15 m and ϕ=35°

Fig. 10 shows comparison plots between the load–displacement curves generated with the proposed *t–z* model and results from two numerical studies. Both investigated suction buckets subjected to tensile loading. Thieken et al. (2014) implemented an advanced hypoplastic soil model and validated it with experimental results obtained by Iskander et al. (1993). Sørensen et al. (2016) used the Mohr-Coulomb constitutive soil model. Reasonable agreement is found with both studies.

It is emphasized that the mathematical models may prove highly inaccurate or become unstable if very small foundation dimensions are given, since the formulation of *t–z* curves is based on statistical analysis of data from numerical models of buckets with diameter and skirt lengths between 10 and 20 m.

CONCLUSIONS

A set of two *t–z* curves for suction buckets are formulated in this paper. These curves describe the behavior of non-linear axial springs that represent friction between bucket skirt and soil. Each formulation relates to a loading direction: tension or compression. The proposed relationships are based on regression analysis of results from 50 finite-element models of suction buckets installed in a typical marine sand. The results of the current research match the ones of other numerical studies to a high degree.

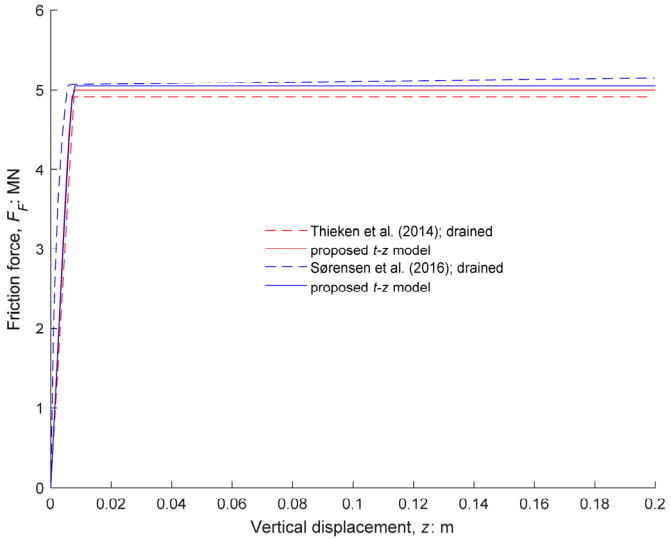

Fig. 10. Load–displacement curves computed with the proposed *t–z* formulation and compared with other numerical studies using equivalent bucket dimensions and soil properties

The static *t–z* curves may be conveniently implemented at the preliminary stages of foundation design, since they require three basic variables as input parameters: bucket diameter, sand's friction angle and initial vertical overburden pressure. Thus, a minimum amount of site-specific data is sufficient for enabling the use of proposed mathematical models. By generating load–displacement curves, practicing engineers may obtain initial estimates of minimum bucket dimensions with respect to fulfilling ULS conditions.

The current study is especially relevant for jacket structures mounted on suction buckets, since the loading patterns are such that the legs may be loaded in tension or compression. An essential feature of the proposed *t–z* curves is their ability to describe the response of suction buckets according to the loading direction.

Modeling geostructures by discretizing the system into springs has found decades-long success within pile design, therefore the presented work does not bring novelty at the conceptual level. Rather, it is the new context of bucket foundations that highlights its uniqueness.

ACKNOWLEDGEMENTS

The authors gratefully acknowledge the financial support received from the European Union under the Horizon 2020 research program. This study is funded as part of i4Offshore project (Integrated Implementation of Industrial Innovations for Offshore Wind Cost Reduction).

REFERENCES

Achmus, M, Kuo, Y-S, and Abdel-Rahman, K (2009). "Behavior of monopile foundations under cyclic lateral load", *Comput Geotech*, 36, 725–735.

Achmus, M, Akdag, CT, and Thieken, K (2013). "Load-bearing behaviour of suction bucket foundations in sand", *Appl Ocean Res*, 43, 157–165.

Achmus, M, and Thieken, K (2014). "Numerical simulation of the tensile resistance of suction buckets in sand", *J Ocean Wind Energ*, 1(4), 231–239.

Achmus, M, and Gütz, P (2016). "Numerical modeling of the behavior of bucket foundations in sand under cyclic tensile loading", *Proc 6th*

Int Conf Struct Eng, Mech and Comp, Cape Town, South Africa, 2085–2091.
API (American Petroleum Institute) (2000). *Recommended practice for planning, designing, and constructing fixed offshore platforms—working stress design*, RP 2A-WSD, 21st ed, American Petroleum Institute, Washington, DC.
Barari, A, and Ibsen, LB (2012). "Undrained response of bucket foundations to moment loading", *Appl Ocean Res*, 36, 12–21.
Barari, A, and Ibsen, LB (2018). "A macro-element approach for non-linear response of offshore skirted footings", *Proc 5th GeoChina Int Conf 2018 – Civil Infrastructures Confronting Severe Weathers and Climate Changes: From Failure to Sustainability*, HangZhou, China, 127–139.
Bohn, C, dos Santos, AL, and Frank, R (2016). "Development of axial pile load transfer curves based on instrumented load tests", *J Geotech Geoenviron Eng*, 143(1), paper 04016081.
Bolton, MD (1986). "The strength and dilatancy of sands", *Géotechnique*, 36(1), 65–78.
Coyle, HM, and Sulaiman, IH (1967). "Skin friction for steel piles in sand", *J Soil Mech Found Division*, ASCE, 93(6), 261–278.
DNV (Det Norske Veritas) (1992). *Foundations. Classification Notes No. 30.4*, Det Norske Veritas, Oslo.
Fleming, WGK (1992). "A new method for single pile settlement prediction and analysis", *Géotechnique* 42(3), 411–425.
Hardin, BO, and Black, WL (1969). "Closure to 'Vibration modulus of normally consolidated clay'". *J Soil Mech Found Division*, ASCE, 95(6), 1531–1537.
Hossain, MS, and Randolph, MF (2009). "New mechanism-based design approach for spudcan foundations on single layer clay", *J Geotech Geoenviron Eng*, 135(9), 1264–1274.
Ibsen, LB, Larsen, KA, and Barari, A (2014). "Calibration of failure criteria for bucket foundations on drained sand under general loading", *J Geotech Geoenviron Eng*, 140(7), paper 04014033.
Iskander, MG, Olson, RE, and Pavlicek, RW (1993). "Behavior of suction piles in sand", in *Design and performance of deep foundations: piles and piers in soil and soft rock* (eds Nelson, PP, Smith, TD, and Clukey, EC), 157–171, ASCE, New York.
Janbu, N (1967). "Settlement calculations based on the tangent modulus concept", *Three guest lectures at Moscow State University. Bulletin No. 2*, Norwegian Institute of Technology, Trondheim.
Kraft, LM Jr, Ray, RP, and Kagawa, T (1981). "Theoretical t–z curves", *J Geotech Eng Division*, ASCE, 107(11), 1543–1561.
Larsen, KA, Ibsen, LB, and Barari, A (2013). "Modified expression for the failure criterion of bucket foundations subjected to combined loading", *Can Geotech J*, 50(12), 1250–1259.
Lombardi, D, Dash, SR, Bhattacharya, S, Ibraim, E, Muir Wood, D, and Taylor, CA (2017). "Construction of simplified design *p–y* curves for liquefied soils", *Géotechnique*, 67(3), 216–227.
Lu, Q, and Luo, Q (2018). "A load transfer approach for studying the load–deformation response of vertically loaded single pile", *Proc 2nd Int Symp on Asia Urban GeoEngineering*, Changsha, China, 369–384.
Mana, DSK, Gourvenec, S, Randolph, MF, and Hossain, MS (2012). "Failure mechanisms of skirted foundations in uplift and compression", *Int J Phys Model Geotech*, 12(2), 47–62.
Mana, DSK, Gourvenec, S, and Randolph, MF (2014). "Numerical modelling of seepage beneath skirted foundations subjected to vertical uplift", *Comput Geotech*, 55, 150–157.
Nanda, S, and Patra, NR (2014). "Theoretical load-transfer curves along piles considering soil nonlinearity", *J Geotech Geoenviron Eng*, 140(1), 91–101.
Nielsen, SK, Shajarati, A, Sørensen, KW, and Ibsen, LB (2012). "Behaviour of dense Frederikshavn sand during cyclic loading", *DCE Technical Memoranda*, 15, Department of Civil Engineering, Aalborg University, Aalborg, Denmark.
Oh, K-Y, Nam, W, Ryu, MS, Kim, J-Y, and Epureanu, BI (2018). "A review of foundations of offshore energy convertors: current status and future perspectives", *Renew Sust Energ Rev*, 88, 16–36.
Østergaard, MU, Knudsen, BS, and Ibsen, LB (2015). "P-y curves for bucket foundations in sand using finite element modeling", *Proc 3rd Int Symp on Frontiers in Offshore Geotechnics*, Oslo, Norway, 343–348.
Park, J-S, Park, D, and Yoo, J-K (2016). "Vertical bearing capacity of bucket foundations in sand", *Ocean Eng*, 121, 453–461.
Park, J-S, and Park, D (2017). "Vertical bearing capacity of bucket foundation in sand overlying clay", *Ocean Eng*, 134, 62–76.
Plaxis (2017). *PLAXIS 2D* Manuals, Plaxis bv, Delft.
Randolph, MF, and Wroth, CP (1978). "Analysis of deformation of vertically loaded piles", *J Geotech Eng Division*, ASCE, 104(12), 1465–1488.
Schanz, T, Vermeer, PA, and Bonnier, PG (1999). "The hardening soil model: formulation and verification", *Proc 1st Int PLAXIS Symp: Beyond 2000 in Computational Geotechnics*, Amsterdam, The Netherlands, 281–296.
Seed, HB, and Reese, C (1957). "The action of soft clay along friction piles", *Transactions ASCE*, 122(1), 731–754.
Shen, K, Zhang, Y, Klinkvort, RT, Sturm, H, Jostad, HP, Sivasithamparam, N, and Guo, Z (2017). "Numerical simulation of suction bucket under vertical tension loading", *Proc 8th Int Conf on Offshore Site Investigation and Geotechnics*, London, UK, 488–497.
Sørensen, ES, Clausen, J, and Damkilde, L (2016). "Comparison of numerical formulations for the modeling of tensile loaded suction buckets", *Comput Geotech*, 83, 198–208.
Thieken, K, Achmus, M, and Schröder, C (2014). "On the behavior of suction buckets in sand under tensile loads", *Comput Geotech*, 60, 88–100.
Tjelta, TI (2015). "The suction foundation technology", *Proc 3rd Int Symp on Frontiers in Offshore Geotechnics*, Oslo, Norway, 85–94.
Vahdatirad, MJ, Troya Diaz, A, Nielsen, S, Ibsen, LB, Andersen, LV, Firouzianbandpey, S, and Griffiths, DV (2016). "A load-displacement based approach to assess the bearing capacity and deformations of mono-bucket foundations", *Proc 6th Int Conf Struct Eng, Mech and Comp*, Cape Town, South Africa, 2105–2111.
Vijayvergiya, VN (1977). "Load–movement characteristics of piles", *Proc 4th Annual Symp of the Waterway, Port, Coastal, and Ocean Division of ASCE*, Long Beach, CA, USA, vol 2, 269–284.
Wang, Z, Xie, X, and Wang, J (2012). "A new nonlinear method for vertical settlement prediction of a single pile and pile groups in layered soils", *Comput Geotech*, 45, 118–126.
Wang, X, Zeng, X, Li, J, Yang, X, and Wang, H (2018). "A review on recent advancements of substructures for offshore wind turbines", *Energ Convers Manage*, 158, 103–119.
Winkler, E (1867). *Die Lehre von der Elasticitaet und Festigkeit.* Dominicus, Prague. In German.
Wolf, TK, Rasmussen, KL, Hansen, M, Roesen, HR, and Ibsen, LB (2013). "Assessment of p–y curves from numerical methods for a non-slender monopile in cohesionless soil", *DCE Technical Memoranda*, 64, Department of Civil Engineering, Aalborg University, Aalborg, Denmark.
Zafeirakos, A, and Gerolymos, N (2016). "Bearing strength surface for bridge caisson foundations in frictional soil under combined loading", *Acta Geotech*, 11(5), 1189–1208.
Zhou, W, Guo, Z, Wang, L, and Rui, S (2019). "Dynamic responses of jacket foundation offshore wind turbine considering the cyclic loading effects", in *Energy Geotechnics, SEG 2018* (eds Ferrari, A, and Laloui, L), 451–458, Springer, Cham.